ChemComm

Chemical Communications

rsc.li/chemcomm

ROYAL SOCIETY
OF CHEMISTRY

COMMUNICATION
Nobuhiro Yanai *et al.*
Guest-responsive coherence time of radical qubits in a
metal–organic framework

60 YEARS
ANNIVERSARY

Check for updates

Guest-responsive coherence time of radical qubits in a metal–organic framework†

Miku Inoue, [ID] [a] Akio Yamauchi, [a] Bhavesh Parmar, [ID] [a] Kana Orihashi, [a] Manpreet Singh, [ID] [a] Mizue Asada, [b] Toshikazu Nakamura [ID] [b] and Nobuhiro Yanai [ID] ★[ac]

Metal–organic frameworks (MOFs) integrated with molecular qubits are promising for quantum sensing. In this study, a new UiO-type MOF with a 5,12-diazatetracene (DAT)-containing ligand is synthesized, and the radicals generated in the MOF exhibit high stability and a relatively long coherence time (T_2) responsive to the introduction of various guest molecules.

Quantum bits (qubits) are the basic units of quantum information science (QIS) and have a higher information processing capability than classical bits because they can take superpositions of quantum states.[1–7] Quantum sensing is one of the applications of qubits to measure physical quantities using quantum effects.[8–12] Quantum sensing, by utilizing the property of superposition states to be sensitive to the external environment, is expected to exhibit higher sensitivity than conventional sensing and have a significant impact on a wide range of fields such as chemistry and biology.[13] The coherence time, evaluated as the spin–spin relaxation time (T_2), is an important parameter directly related to the sensitivity of quantum sensing.[10] Nitrogen vacancy (NV) centers in diamond are representative quantum sensors because they exhibit long T_2 from microseconds to milliseconds even at room temperature,[13,14] but it is difficult to precisely control their defect positions and structures.[3,15] On the other hand, molecular qubits,[4,7,8] which utilize the unpaired electron spins of molecules, can be structurally defined at the atomic level, and their properties can be finely controlled by changing the molecular structure.

Metal–organic frameworks (MOFs) provide an ideal platform for quantum sensing using molecular qubits.[9,16–24] Qubits can be integrated into MOFs during or after synthesis. Paramagnetic metal ions[16,17,19,23] and organic molecules[9,21,22,24] in doublet, triplet, and quintet states have been introduced into MOFs as qubits. For the potential of chemical quantum sensing, the interactions between adsorbed guest molecules and qubits can be understood by estimating relaxation time and hyperfine interactions with electron spin resonance (ESR) measurements.[9,20] We have previously reported that MOFs consisting of pyridyl-modified 5,12-diazatetracene (DAT) ligands (DPyDAT) and Zn ions undergo charge separation from the photo-excited DAT chromophore, and that the resulting DAT radicals exhibit relatively long coherence times T_2.[21,24] However, due to the instability of the MOF structure, the response of T_2 to various guest molecules could not be evaluated.

In this work, we newly synthesize a highly porous rigid MOF, named DAT-MOF-4, using a DAT-based dicarboxylate ligand, and demonstrate the guest responsivity of DAT radical qubits (Fig. 1). DAT radicals in DAT-MOF-4 are found to be stable at room temperature. The rigid structure of DAT-MOF-4 with UiO-68 topology[25] enables the stable introduction of the guest molecules. The densely packed DAT in the rigid UiO-type structure suppresses the electron spin relaxation, giving a relatively long T_2 value of 0.56 μs in the absence of guest

a Department of Applied Chemistry, Graduate School of Engineering, Kyushu University, 744 Moto-oka, Nishi-ku, Fukuoka 819-0395, Japan. E-mail: yanai@mail.cstm.kyushu-u.ac.jp

b Institute for Molecular Science, Nishigonaka 38, Myodaiji, Okazaki 444-8585, Japan

c CREST, JST, Honcho 4-1-8, Kawaguchi, Saitama 332-0012, Japan

† Electronic supplementary information (ESI) available: Detailed experimental procedures, ^{1}H-NMR spectrum, MALDI-TOF-MS spectrum, ESR and pulse ESR data. See DOI: https://doi.org/10.1039/d4cc01564a
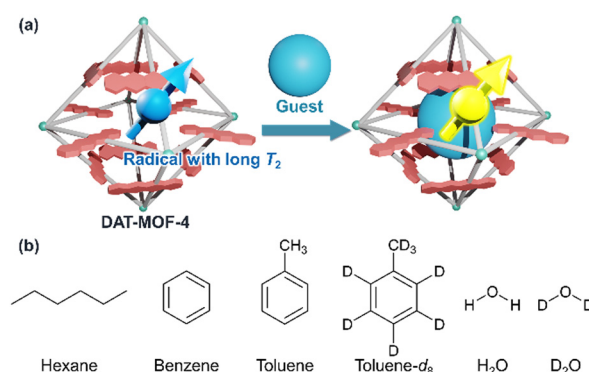

Fig. 1 (a) Schematic illustration of quantum sensing by radicals with long coherence time (T_2) in MOFs. (b) Guest molecules used in this research.

molecules. The T_2 value of radicals shows some response upon guest inclusion, showing the possibility of quantum chemosensing.

4,4′-(Benzo[*b*]phenazine-6,11-diyl)dibenzoic acid (DATDBA) was synthesized following the reported procedure (Fig. S1 and S2, ESI†).[26] DAT-MOF-4 was synthesized *via* a solvothermal reaction of ZrCl$_4$ with DATDBA in the presence of trifluoroacetic acid as a modulator in DMF at 120 °C for 72 h (Fig. 2a). The structure and phase purity of DAT-MOF-4 were confirmed by powder X-ray diffraction (PXRD) (Fig. 2b). The experimental powder pattern was matched with the simulated UiO-68, confirming that DAT-MOF-4 has the same topology as UiO-68.[25]

In contrast to our previous DAT-based MOFs, DAT-MOF-4 showed very good structural stability. Thermogravimetric analysis (TGA) of the as-synthesized DAT-MOF-4 showed that guest molecules were desorbed by around 130 °C and the MOF structure was stable up to 450 °C (Fig. 2d). DAT-MOF-4 was activated by removing guest DMF molecules through solvent exchange with chloroform at room temperature and drying by heating at 120 °C under vacuum. Importantly, the activated DAT-MOF-4 showed a PXRD pattern similar to that of as-synthesized DAT-MOF-4, indicating that the structural integrity is maintained after guest removal. The porosity and high surface area of the framework was also confirmed by the N$_2$ gas adsorption measurements of activated DAT-MOF-4 at 77 K (Fig. 2c). DAT-MOF-4 showed the IUPAC type-I adsorption isotherm, which is characteristic of microporous materials. The Brunauer–Emmett–Teller (BET) surface area was calculated to be 1790 m^2 g^{-1} and the average pore size was estimated to be 1.1 nm by the non-local density functional theory (NLDFT) model analysis.

In our previous study, we observed that in three mixed-linker MOFs (DAT-MOF-1, 2, and 3) consisting of Zn ions, DPyDAT,
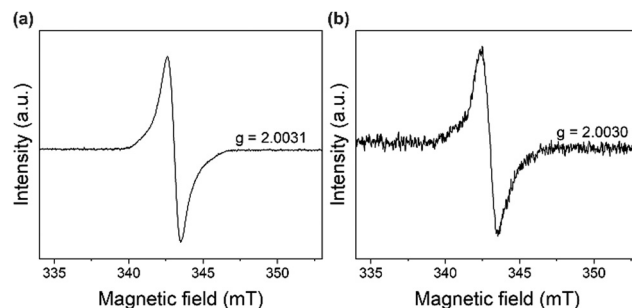

Fig. 3 CW-ESR spectra of (a) activated DAT-MOF-4 and (b) DATDBA crystals dispersed in paraffin oil, which was added to protect the sample. The microwave frequency of each measurement was (a) 9.617631 GHz and (b) 9.616428 GHz, respectively.

and different co-ligands, photoirradiation induces the charge separation and the formation of DAT radical cations.[21,24] However, in the current DAT-MOF-4, the laser irradiation did not bring any increase of the ESR signal intensity. Meanwhile, even without light irradiation, continuous wave (CW)-ESR measurements of DAT-MOF-4 in the "dark" condition showed an ESR signal similar to the previously-observed ESR signal of DAT radicals (Fig. 3a and Fig. S3, ESI†). The radical signal in DAT-MOF-4 was found to be stable for several days. In previous literature, a similar radical-derived ESR signal was reported from a simple molecular crystal of DAT.[27] The ESR signal did not disappear after sublimation purification of DAT and was best modeled when hyperfine coupling with ^{14}N is considered, and the authors concluded that the radicals are derived from DAT itself, not from impurities.[27] Although the details of the generation mechanism of the DAT radicals have not been fully understood, similar radical generation would also take place in the current DAT-MOF-4. The *g* value of the radical in DAT-MOF-4 was 2.0031, which is comparable to our previously reported DAT radical cation,[21,24] also supporting the formation of DAT radicals in DAT-MOF-4. In our previous report on another MOF (DAT-MOF-1) with a DAT derivative as a ligand, we performed Rabi oscillation experiments and identified it as radical species with $S = 1/2$ by comparing the oscillation frequency with photoexcited triplet species.[24] Furthermore, a similar ESR signal was observed from the molecular crystals of ligand DATDBA, which also supports that the radical in DAT-MOF-4 is derived from the DAT-based ligand (Fig. 3b). We also tried to measure the ESR of the ligand solution at the highest possible concentration. From the concentration dependence of the absorbance of the THF solution of the ligand, we found that up to 1 mM, the ligand is in a molecular dispersion state (Fig. S4, ESI†). We performed ESR measurements of 1 mM ligand solution with many integrations (2000 times). The ESR signal with hyperfine splitting was observed from the ligand solution (Fig. S5, ESI†), confirming that the origin of the radical is the DAT radical.

By taking advantage of the rigid porous structure of DAT-MOF-4, the following six guest molecules were introduced into activated DAT-MOF-4 through the vapor phase at saturated vapor pressure at room temperature: hexane, benzene, toluene,
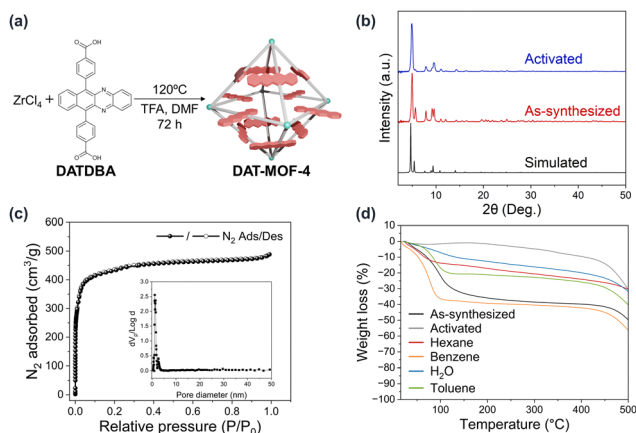

Fig. 2 (a) Synthetic scheme of DAT-MOF-4. (b) Simulated PXRD pattern of UiO-68 (black line) and experimental PXRD patterns of the as-synthesized DAT-MOF-4 (red line) and activated DAT-MOF-4 (blue line). (c) N$_2$ adsorption (filled circles) and desorption (open circles) isotherm for DAT-MOF-4 at 77 K. Inset: Pore-size distribution plot of DAT-MOF-4. (d) TGA curves of the as-synthesized DAT-MOF-4 (black line), activated DAT-MOF-4 (grey line), and DAT-MOF-4 exposed to hexane (red line), benzene (orange line), H$_2$O (light blue line), and toluene (light green line) vapor. Measurements were carried out under N$_2$ with a heating rate of 10 °C min^{-1}.

H_2O, toluene-d_8, and D_2O. The adsorption of these guest molecules in DAT-MOF-4 was confirmed by TGA measurements (Fig. 2d). CW-ESR measurements showed no significant change in g value of DAT-MOF-4 by the guest accommodation (Fig. S6, ESI†). To evaluate the guest dependence of the quantum coherence of the radicals, the coherence time T_2 was estimated by pulsed ESR measurements with the spin echo sequence at room temperature (Fig. 4). The T_2 values were obtained from the decay constants of mono-exponential fits of the echo signal decays. A relatively long T_2 value of 0.56 µs was observed for activated DAT-MOF-4, which is close to the T_2 values of previous DAT-MOF-1, 2, 3.[21,24] By the adsorption of hexane, toluene and H_2O, T_2 values became shorter to 0.49 µs, 0.44 µs and 0.43 µs, respectively. Meanwhile, DAT-MOF-4 with deuterated solvents, toluene-d_8 and D_2O, showed longer T_2 of 0.62 µs and 0.70 µs, respectively. These results show that T_2 of radicals in MOFs can be responsive to the chemical stimuli.

The spin–lattice relaxation time T_1 determined by the inversion recovery sequence of pulsed ESR measurements was sufficiently longer than T_2 for any guest included, indicating that T_2 is not limited by T_1 (Fig. S7, ESI†). By using a standardized ESR sample (TEMPO in toluene) as a reference, 0.03 mol% of DAT ligand in DAT-MOF-4 is estimated to be present as radicals, and the average distance between radicals is about 17 nm (Fig. S8, ESI†). This means that the effect of spin–spin interaction on T_2 in the current MOF system is negligibly small.[23] There are at least two other possible factors that affect T_2. The first is the hyperfine coupling between electron spins and nuclear spins. It is known that the quantum coherence of electron spins can be influenced by nuclear spins with large gyromagnetic ratio such as protons.[10,15] When guests were introduced into the pores, the DAT radicals can be close to such spins, and hyperfine interactions between radical

electron spins and nuclear spins induce the spin relaxation. This may be observed in the case of DAT-MOF-4 containing hexane, toluene, and H_2O. Another factor is the suppression of the radical mobility by the adsorbed guest molecules. The local magnetic field around radicals can fluctuate by the motion of DAT ligands, which causes the decoherence.[15] This molecular motion may be suppressed by the presence of guest molecules in the MOF. Longer T_2 values were obtained with the deuterated solvents, toluene-d_8 and D_2O, compared with the activated samples and the ones with protonated guests. Since ^2D has a gyromagnetic ratio six times smaller than ^1H, the relaxation caused by hyperfine coupling was suppressed, and the effect of the motional restriction might be dominant. In the case of the DAT-MOF-4 with benzene, the T_2 value was almost similar to that of the activated sample. This might be because of the two competing effects, enhanced relaxation by the hyperfine coupling and suppressed relaxation by the restriction of molecular motion, were comparable in the case of benzene.

In conclusion, we have developed MOF containing radical qubits that can be utilized for quantum sensing. By constructing MOFs with ligands containing the DAT moiety, stable DAT radicals could be generated in the MOFs. The long coherence time T_2 of the radicals was obtained by densely accumulating DAT in the rigid UiO-framework. Furthermore, the response of T_2 to various guest molecules suggests that the hyperfine interaction between the electron spins of the radicals and the nuclear spins of the guest molecules as well as the mobility of the radical qubits are important controlling factors. The method developed in this study is very simple, using DAT-containing ligands to construct MOFs, and is expected to be applied to various MOF structures in the future to construct libraries that show different responses to a wider variety of target analytes at different analyte concentrations.
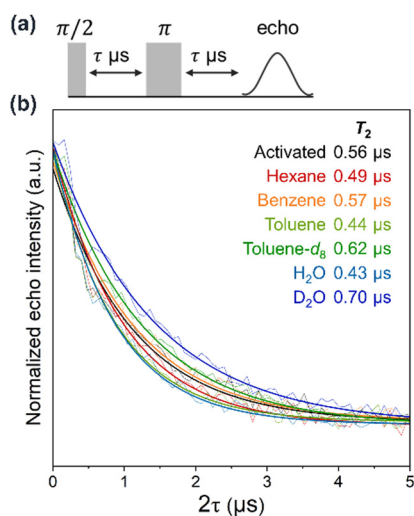
Fig. 4 (a) Hahn-echo sequence of pulsed ESR measurements. (b) Decay of the echo intensity of the Hahn-echo sequence for activated DAT-MOF-4 (black line), and DAT-MOF-4 with hexane (red line), benzene (orange line), toluene (light green line), toluene-d_8 (green line), H_2O (light blue line), and D_2O (blue line) at room temperature. Single-exponential fitting curves for the decay signal and resulting T_2 values are also shown.

Conflicts of interest

There are no conflicts to declare.

References

1 N. W. Hendrickx, W. I. L. Lawrie, L. Petit, A. Sammak, G. Scappucci and M. Veldhorst, *Nat. Commun.*, 2020, **11**, 3478.

2 J. M. Gertler, B. Baker, J. Li, S. Shirol, J. Koch and C. Wang, *Nature*, 2021, **590**, 243–248.

3 M. R. Wasielewski, M. D. E. Forbes, N. L. Frank, K. Kowalski, G. D. Scholes, J. Yuen-Zhou, M. A. Baldo, D. E. Freedman, R. H. Goldsmith, T. Goodson, M. L. Kirk, J. K. McCusker, J. P. Ogilvie, D. A. Shultz, S. Stoll and K. B. Whaley, *Nat. Rev. Chem.*, 2020, **4**, 490–504.

4 S. Zhou, J. Yuan, Z. Y. Wang, K. Ling, P. X. Fu, Y. H. Fang, Y. X. Wang, Z. Liu, K. Porfyrakis, G. A. D. Briggs, S. Gao and S. D. Jiang, *Angew. Chem., Int. Ed.*, 2022, **61**, e202115263.

5 M. L. Kirk, D. A. Shultz, J. Chen, P. Hewitt, D. Daley, S. Paudel and A. van der Est, *J. Am. Chem. Soc.*, 2021, **143**, 10519–10523.

6 T. Quintes, M. Mayländer and S. Richert, *Nat. Rev. Chem.*, 2023, **7**, 75–90.

7 S. Gorgon, K. Lv, J. Grune, B. H. Drummond, W. K. Myers, G. Londi, G. Ricci, D. Valverde, C. Tonnele, P. Murto, A. S. Romanov, D. Casanova, V. Dyakonov, A. Sperlich, D. Beljonne, Y. Olivier, F. Li, R. H. Friend and E. W. Evans, *Nature*, 2023, **620**, 538–544.

8 C.-J. Yu, S. von Kugelgen, D. W. Laorenza and D. E. Freedman, *ACS Cent. Sci.*, 2021, **7**, 712–723.

9 L. Sun, L. Yang, J.-H. Dou, J. Li, G. Skorupskii, M. Mardini, K. O. Tan, T. Chen, C. Sun, J. J. Oppenheim, R. G. Griffin, M. Dincă and T. Rajh, *J. Am. Chem. Soc.*, 2022, **144**, 19008–19016.

10 C. E. Jackson, I. P. Moseley, R. Martinez, S. Sung and J. M. Zadrozny, *Chem. Soc. Rev.*, 2021, **50**, 6684–6699.

11 C. L. Degen, F. Reinhard and P. Cappellaro, *Rev. Mod. Phys.*, 2017, **89**, 035002.

12 M. Atzori and R. Sessoli, *J. Am. Chem. Soc.*, 2019, **141**, 11339–11352.

13 T. Zhang, G. Pramanik, K. Zhang, M. Gulka, L. Wang, J. Jing, F. Xu, Z. Li, Q. Wei, P. Cigler and Z. Chu, *ACS Sens.*, 2021, **6**, 2077–2107.

14 J. R. Maze, P. L. Stanwix, J. S. Hodges, S. Hong, J. M. Taylor, P. Cappellaro, L. Jiang, M. V. G. Dutt, E. Togan, A. S. Zibrov, A. Yacoby, R. L. Walsworth and M. D. Lukin, *Nature*, 2008, **455**, 644–647.

15 Y. Qiu, H. J. Eckvahl, A. Equbal, M. D. Krzyaniak and M. R. Wasielewski, *J. Am. Chem. Soc.*, 2023, **145**, 25903–25909.

16 M. J. Jellen, M. J. Ayodele, A. Cantu, M. D. E. Forbes and M. A. Garcia-Garibay, *J. Am. Chem. Soc.*, 2020, **142**, 18513–18521.

17 A. Kultaeva, A. Pöppl and T. Biktagirov, *J. Phys. Chem. Lett.*, 2022, **13**, 6737–6742.

18 M. J. Graham, J. M. Zadrozny, M. S. Fataftah and D. E. Freedman, *Chem. Mater.*, 2017, **29**, 1885–1897.

19 J. M. Zadrozny, A. T. Gallagher, T. D. Harris and D. E. Freedman, *J. Am. Chem. Soc.*, 2017, **139**, 7089–7094.

20 A. Yamauchi, S. Fujiwara, N. Kimizuka, M. Asada, M. Fujiwara, T. Nakamura and N. Yanai, *ChemRxiv*, 2022, DOI: **10.26434/chemrxiv-2022-4hnsj**.

21 K. Orihashi, A. Yamauchi, M. Inoue, B. Parmar, S. Fujiwara, N. Kimizuka, M. Asada, T. Nakamura and N. Yanai, *Dalton Trans.*, 2024, **53**, 872–876.

22 A. Yamauchi, K. Tanaka, M. Fuki, S. Fujiwara, N. Kimizuka, T. Ryu, M. Saigo, K. Onda, R. Kusamoto, N. Ueno, Y. Kobori, K. Miyata and N. Yanai, *Sci. Adv.*, 2024, **10**, eadi3147.

23 C.-J. Yu, S. von Kugelgen, M. D. Krzyaniak, W. Ji, W. R. Dichtel, M. R. Wasielewski and D. E. Freedman, *Chem. Mater.*, 2020, **32**, 10200–10206.

24 K. Orihashi, A. Yamauchi, S. Fujiwara, M. Asada, T. Nakamura, J. Ka-Ho Hui, N. Kimizuka, K. Tateishi, T. Uesaka and N. Yanai, *J. Am. Chem. Soc.*, 2023, **145**, 27650–27656.

25 J. H. Cavka, S. Jakobsen, U. Olsbye, N. Guillou, C. Lamberti, S. Bordiga and K. P. Lillerud, *J. Am. Chem. Soc.*, 2008, **130**, 13850–13851.

26 H. Kouno, K. Orihashi, K. Nishimura, Y. Kawashima, K. Tateishi, T. Uesaka, N. Kimizuka and N. Yanai, *Chem. Commun.*, 2020, **56**, 3717–3720.

27 M. Attwood, D. K. Kim, J. H. L. Hadden, A. Maho, W. Ng, H. Wu, H. Akutsu, A. J. P. White, S. Heutz and M. Oxborrow, *J. Mater. Chem. C*, 2021, **9**, 17073–17083.